Biophys Struct Mech (1984) 10: 185–196

Biophysics
of Structure
and Mechanism

Conductivities and Anisotropies in Diffusely Arranged Nervous Tissues; Their Determination and Importance in Neurophysiological Studies*

J. Breckow and A. Keuper

Fachbereich Biologie, Philipps-Universität, D-3550 Marburg, Federal Republic of Germany

Abstract. A new method for conductivity measurements in nervous tissues is introduced. A multi-electrode device is used for successive current injections and simultaneous potential recordings, which improves statistical evidence. A procedure to investigate anisotropies in nervous tissue is theoretically developed and experimentally applied to the thoracic ganglia of the migratory locust *Locusta migratoria.* The region around the frontal acoustic neuropile of the metathoracic ganglion exhibits a very slight anisotropy. Its preference direction is represented by the animal's body longitudinal axis. In the mesothoracic ganglion no anisotropy at all was revealed. Inhomogenities could not be found within the nervous tissue investigated. These results are discussed with respect to neurophysiological investigations.

Key words: Conductivity in nervous tissues – Anisotropy – Inhomogenity – Multi-electrode recording

Introduction

In certain neurophysiological investigations it is necessary to obtain detailed information about the electrical properties of the nervous tissue investigated. In particular, the conductivity conditions are often of interest. To avoid wrong interpretation of extracellular recordings of neuronal ensemble activities, the underlying current flows dependent on certain conductivity properties of a given system have to be considered. Such a consideration is required for instance for field potential analysis and current density or current source density investigations (Nicholson 1973; Kwan and Murphy 1974; Nicholson and Freeman 1975; Freeman and Nicholson 1975).

In vertebrates, some techniques for measuring resistivities or conductivities are available (e.g., Freeman and Stone 1969; Kwan and Murphy 1974; Nicholson

---

* Supported by the Deutsche Forschungsgemeinschaft as part of the program "Codierungsleistungen der Insektenhörbahn" (Ka 498/3-2)

and Freeman 1975; Yedlin et al. 1974) but little is known about these aspects with regard to insects' nervous tissues, e.g., such diffusely but complex arranged structures like the dendritic regions (neuropiles).

This paper reports new theoretical and experimental approaches and their application to the thoracic ganglia of the migratory locust *Locusta migratoria.*

Material and Methods

1. Theoretical

1.1. Conductivity Tensor. The conductivity σ is a (linear) operator in the most general expression of Ohm's Law:

$$\vec{\mathbf{j}} = \sigma \vec{\mathbf{E}} \tag{1}$$

$\vec{\mathbf{j}}$: Current flow density

$\vec{\mathbf{E}}$: Electrical field

This generally asymmetric second-rank tensor is in the three-dimensional case a 3 × 3 matrix:

$$\sigma = (\sigma_{ik}) \quad i, k = 1, 2, 3 \tag{2}$$

σ can be reduced to a symmetric tensor, i.e., the diminuation of independent components from 9 to 6 (if rot $\vec{\mathbf{E}} = \vec{\mathbf{0}}$):

$$\sigma_{ik} = \sigma_{ki} \tag{3}$$

(Landau and Lifschitz 1960).

The tensor σ can be transformed – as each symmetric second-rank tensor – to a diagonal form by choosing adequate coordinate axes (Morse and Feshbach 1963). That is, the off-diagonal elements $\sigma_{ik}, i \neq k$ vanish.

1.2. Main Axes Transformation. In the case of non-degeneration, the tensor still has in its diagonal form three independent components σ_{11}, σ_{22}, σ_{33} ($\sigma_{ik} = 0$, if $i \neq k$). The Eigen vectors associated with these Eigen values form an orthogonal system independent of the symmetric properties of the medium. Thus, this orthogonal system determines the axes of the coordinate system:

$$\vec{\mathbf{j}} = \sum_{i=1}^{3} \sigma_i E_i \vec{\mathbf{e}}_i \tag{4}$$

$\vec{\mathbf{e}}_i$: unit vector in i direction.

If either $\vec{\mathbf{j}}$ or $\vec{\mathbf{E}}$ is parallel to one of these axes, then the directions of $\vec{\mathbf{j}}$ and $\vec{\mathbf{E}}$ are identical. This is not valid for one of the vectors $\vec{\mathbf{j}}$ or $\vec{\mathbf{E}}$ having components in various directions.

If a given medium to which a coordinate system is to be associated exhibits a rectangular symmetry due to anatomical or structural features these directions can be supposed to be the wanted coordinate axes (Nicholson and Freeman 1975; Yedlin et al. 1974).

Difficulties arising due to the fact that such principal axes are not known or are not rectangular can be overcome by means of the following approach:

Any symmetric tensor has a number of invariants, i.e., magnitudes independent of the actual coordinate system. Such invariants are:

$$
\begin{aligned}
I_1 &= \sigma_{11} + \sigma_{22} + \sigma_{33} \\
I_2 &= \sigma_{11} \cdot \sigma_{22} + \sigma_{22} \cdot \sigma_{33} + \sigma_{33} \cdot \sigma_{11} - (\sigma_{12}^2 + \sigma_{23}^2 + \sigma_{31}^2) \qquad (5) \\
I_3 &= \mathrm{Det}\,|\sigma|
\end{aligned}
$$

(Joos 1977).

If the diagonal elements σ_{ii} in any direction can be determined and if furthermore one axis is fixed, a rotation around this axis with an angle θ yields $\sigma_{ii}(\theta)$. From this follows:

$$\sigma_{11}(\theta) + \sigma_{22}(\theta) = \text{const}$$

and

$$\sigma_{11}(\theta) \cdot \sigma_{22}(\theta) + \text{const} - \tilde{\sigma} = \text{const}$$

with

$$
\begin{aligned}
&\tilde{\sigma} := \sigma_{12}^2 + \sigma_{23}^2 + \sigma_{31}^2 \\
&\Rightarrow \sigma_{11}(\theta) \cdot \sigma_{22}(\theta) - \tilde{\sigma}(\theta) = \text{const.} \qquad (6)
\end{aligned}
$$

It holds that $\tilde{\sigma}(\theta_0) = 0$ if main axes transformation ($\theta = \theta_0$), otherwise $\tilde{\sigma}(\theta) > 0$. Thus, the coordinate system yielding the diagonal form ($\sigma_{ik} = 0, i \neq k$) is present if the product $\sigma_{11}(\theta_0) \cdot \sigma_{22}(\theta_0)$ becomes minimal. If no such principal axes are present, i.e., the tissue is found to be isotropic ($\sigma_x = \sigma_y = \sigma_z$), a coordinate system can be chosen arbitrarily. Hence, the tensor σ is reduced to a scalar value.

1.3. Conductivity Measurement. The potential φ generated by a point current source at $\vec{\mathbf{x}}_0$ is a function of the conductivity conditions, current intensity I and the distance to the source:

$$\varphi = \varphi(I, \sigma_i, \vec{\mathbf{x}} - \vec{\mathbf{x}}_0) \qquad (7)$$

For a homogeneous, anisotropic and infinite medium φ is given by

$$\varphi(\vec{\mathbf{x}}) = \frac{I}{4\pi}\left(\sum_{i=1}^{3} \alpha_i \cdot \Delta x_i^2\right)^{-1/2} \qquad (8)$$

with

$$\alpha_i := \prod_{\substack{j=1 \\ i \neq j}}^{3} \sigma_j$$

and

$$\Delta x_i := x_i - x_{0i} \quad i = 1, 2, 3 \tag{9}$$

(in the present context: $x_1 =: x$; $x_2 =: y$; $x_3 =: z$)
(Yedlin et al. 1974).

If a current of known magnitude is applied at $\vec{\mathbf{x}}_0$ and $\varphi(\vec{\mathbf{x}})$ is measured at m points of space ($m \geqslant 3$) the conductivity components σ_i can be separated and determined.

The statistical evidence can be greatly improved if all the recording points $\vec{\mathbf{x}}_l$, $l = 1 \ldots m$ are successively also used for current injection $\vec{\mathbf{x}}_n$, $n = 1 \ldots m$, whereas the potentials are measured at the remaining points $\vec{\mathbf{x}}_l \neq \vec{\mathbf{x}}_n$.

The following proportionality holds [cf. Eq. (8)]:

$$\frac{1}{\varphi^2(\vec{\mathbf{x}})} =: f(\Delta x_i^2) \sim \sum_{i=1}^{3} \alpha_i \Delta x_i^2 \tag{10}$$

Let the α_i be determined by

$$Q(\alpha_i) := \sum_{k=1}^{n} \left(\sum_{i=1}^{3} \alpha_i \Delta x_{ik}^2 - f_k \right)^2 \tag{11}$$

to become minimal according to a mean squared distance expression. Therefore the following has to be fulfilled:

$$\operatorname{grad} Q(\alpha_i) \overset{!}{=} \vec{\mathbf{0}} \tag{12}$$

The resulting equation system represents a matrix equation:

$$(a_{ij})\, \vec{\alpha} = \vec{\mathbf{b}} \tag{13}$$

with

$$a_{ij} := \sum_{k=1}^{3} \Delta x_{ik}^2 \cdot \Delta x_{jk}^2 \,.$$

and

$$b_i := \sum_{k=1}^{n} \Delta x_{ik}^2 \cdot f_k \,.$$

The solutions of Eq. (13) are:

$$\alpha_1 = \frac{\begin{vmatrix} b_1 & a_{12} & a_{13} \\ b_2 & a_{22} & a_{23} \\ b_3 & a_{32} & a_{33} \end{vmatrix}}{\operatorname{Det}|a_{ij}|} \qquad \text{etc.} \tag{14}$$

Thus, the conductivity components σ_i can be derived by transforming Eq. (9) to:

$$\sigma_i = \left(\frac{1}{\alpha_i} \prod_{\substack{j=1 \\ j \neq 1}}^{3} \alpha_j\right)^{1/2} \tag{15}$$

2. *Experimental*

All experiments were performed using adults of both sexes of the migratory locust *Locusta migratoria.* Legs and wings were removed. The animals were fixed upside down to a stand by means of a wax colophonium mixture. The nervous tissue of the meso-(Th_2) and of the metathoracic ganglion (Th_3) was investigated. The ganglion to be investigated was then exposed ventrally and the perineurum removed at the recording site. Glass micropipettes with a resistance of 5–15 MΩ were filled with 3 M KCl.

For the precise spatial adjustment of the electrode tips a micromanipulator was constructed which allowed both the movement of each electrode individually towards each other in all dimensions and the positioning of the tips in a spatial lattice according to Fig. 1. Subsequently, the electrodes were glued together at the shoulder regions. This rigidly connected multi-electrode system was introduced into the nervous tissue by a micromanipulator (cf. Breckow et al. 1982).

The electrode spacing was generally chosen as $h = 50$ µm. The penetration axis was the z- (dorso-ventral) direction (Fig. 2). A constant current pulse (10^{-7} A; 200 ms) was applied successively through each of the electrodes (WP Instruments, Micro-Probe System, Model M707), while the potentials generated by this current were measured using the other six electrodes. Thus, by consecutive current injection through all the ($m = 7$) electrodes up to 42 [$= m \cdot (m - 1)$] values were obtained for each recording position of the multi-electrode from which the conductivity components σ_x, σ_y, σ_z could be computed. For computer calculations a PDP 8 was used.

Control experiments were performed in a NaCl-solution [concentration $c = 10^{-4}$ mol/cm^3; conductivity $\sigma = (9.0 \pm 0.7)$ mS/cm] using double-electrode arrangements with various electrode spacing to prove the measuring equipment and to exclude artefacts.

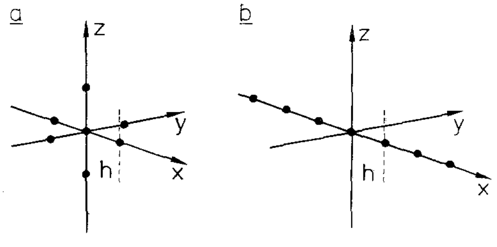

Fig. 1a and b. Schematic presentation of the electrode arrangements and the correlated coordinate system. **a** Three-dimensional cubic alignment; **b** One-dimensional linear alignment

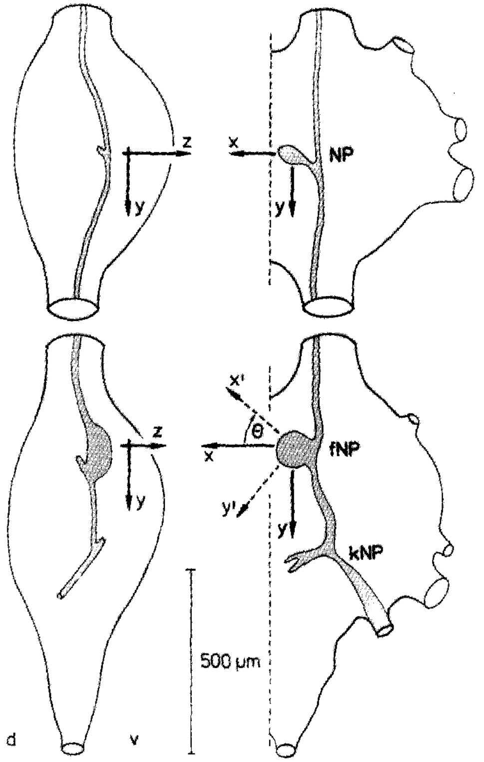

Fig. 2. Schematic presentation of the central projections of the receptor axons of the tympanic organ within the mesothoracic (Th_2) and the metathoracic (Th_3) ganglion. Alignment of a coordinate system. Coordinate rotation around the z-axis (dashed symbols) fNP: frontal acoustic neuropile; kNP: caudal acoustic neuropile. *Left side:* lateral view (*d:* dorsal, *v:* ventral); *right side:* ventral view

Results

1. Preliminary Experiments

Ohm's Law is only valid under certain preconditions. These were investigated in a set of preliminary experiments:

a) Experiments similar to those described by Freeman and Stone (1969) revealed no potential dependence of the conductivities. Thus, the system is supposed to be linear.

b) Since neural tissues may exhibit capacitative properties the electrical conductivity is, in general, frequency dependent. We did not find any frequency dependence at least up to 2 kHz.

c) The electrical properties remained approximately stable over a reasonable period of experimental time. Only a very slight decrease of conductivity in the order of magnitude of about 10% over half an hour was found, due to the tissue drying up.

2. Main Axes Determination

The nervous tissue around the region of the acoustic neuropiles of the meso- and metathoracic ganglia exhibits no apparent directional orientation of structure

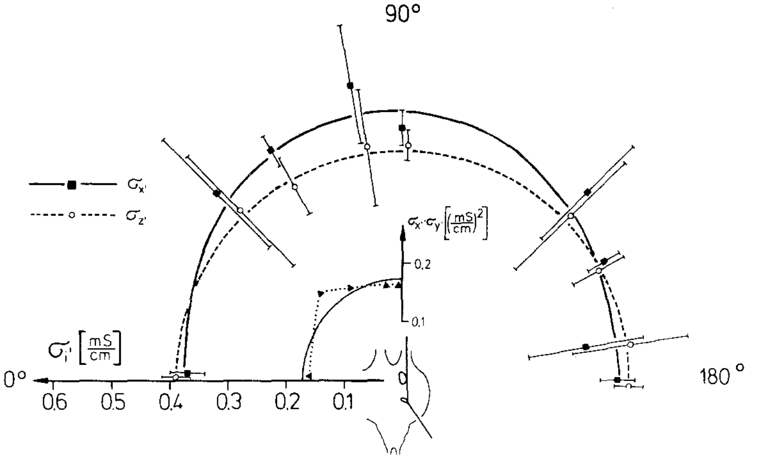

Fig. 3. Polar coordinate diagram of the conductivity components $\sigma_{x'}$ and $\sigma_{z'}$ as a function of the rotation angle θ. The curves represent the fitted linear regressions of $\theta_{x'}$ ($r^2 = 0.72$ with a maximum at $\theta = 85°$) and $\sigma_{z'}$ ($r^2 = 0.99$). The product $\sigma_{x'} \cdot \sigma_{y'}$ is indicated in the range of $0° \leqslant \theta \leqslant 90°$. The solid curve represents values taken from the smoothed curve of $\sigma_{x'}$; the dotted curve is obtained from the measured mean values. The inset indicates schematically the relative site of the ganglion with respect to the angle θ

which would determine an alignment of an "intrinsic" coordinate system from the outset. Morphological investigations have revealed only a very slight arrangement of layers in the XY-plane (Fig. 2) of the acoustic receptor fiber branches in this area. This would mean a weak preference in the dorso-ventral *(z-)* direction. Thus, the determination of possible preference directions in the XY-plane – i.e., the principal axes with respect to the orthogonal system according to Eq. (4) – has to be done by coordinate rotation described in Methods Sect. 1.2. This rotation is performed around the *z*-axis in the direction of the mathematically negative sense (Fig. 2). An electrode arrangement as shown in Fig. 1a was used.

The measurements of $\sigma_{x'}$, $\sigma_{y'}$, $\sigma_{z'}$ yield only the diagonal elements of the conductivity tensor, whereas the σ_{ik}, $i \neq k$ are not considered (if no main axes transformation is present). Thus, generally σ_i depend on the rotation angle θ.

Main axes transformation is given if $\sigma_{x'}(\theta) \cdot \sigma_{y'}(\theta)$ becomes minimal. σ_z should remain constant. Because the electrode arrangement is rectangular, the relationship holds (Fig. 2):

$$\sigma_{y'}(\theta) = \sigma_{x'}(\theta + 90°)\,. \tag{16}$$

Figure 3 shows the results obtained from recordings made within the metathoracic ganglion. Twelve measurements were made at $\theta = 0°$, 6 at $\theta = 60°$, 2 at $\theta = 80°$ and one measurement yielded conductivities at $\theta = 45°$. A slight conductivity maximum is seen at $\theta = 85°$, i.e., roughly in the *y*-direction. The solid curve illustrates the linear regression approximation ($r^2 = 0.72$). $\sigma_{z'}$ is nearly independent of θ ($r^2 = 0.99$). Figure 3 also shows the product $\sigma_{x'} \cdot \sigma_{y'}$.

The dotted line is derived from the measured mean $\sigma_{x'}$-values. The solid line represents values taken from the linear regression curve of $\sigma_{x'}$. The latter suggests isotropy, whereas the products taken from the measured mean values reveal a minimum at about $\theta = 0°$ and $\theta = 90°$, respectively. This would mean directional preference in the x- and y-direction aligned as in Fig. 2. Measurements made in the mesothoracic ganglion (Th_2) revealed no main directional preference at all.

3. Conductivity Measurements

In addition to the cubic electrode arrangement (Fig. 1a) for detailed conductivity measurements, the electrode configuration illustrated in Fig. 1b was also used. Generally, the latter allows a variation of the measuring distance $\Delta x = x - x_0$ between 50 µm and 300 µm for the same positioning of the electrode set. However, only electrode spacings Δx of $h = 50$ µm and $2\,h = 100$ µm between current injection electrode and potential measuring electrode were taken for evaluating the conductivity values. Greater distances would possibly lead to erroneous results since surface boundary effects cannot be neglected any more (see Discussion). The mean values of all conductivity measurements are:

Mesothoracic ganglion (Th_2) measured in 25 animals:
$\sigma_x = (0.42 \pm 0.06)$ mS/cm,
$\sigma_y = (0.42 \pm 0.06)$ mS/cm,
$\sigma_z = (0.42 \pm 0.04)$ mS/cm.

Metathoracic ganglion (Th_3) measured in 30 animals:
$\sigma_x = (0.37 \pm 0.03)$ mS/cm,
$\sigma_y = (0.43 \pm 0.03)$ mS/cm,
$\sigma_z = (0.39 \pm 0.04)$ mS/cm.

4. Inhomogenities

To find out any inhomogenities within the tissue ($d\sigma/d\vec{x} \neq 0$) the electrode arrangement shown in Fig. 1b was applied using only potential values obtained from the adjacent electrode to the current electrode. Thus, $\Delta x = \text{const} = 50$ µm. In general, each expression of $d\sigma_i/dx_j\ i, j = 1, 2, 3$ exists independently, therefore each one must be considered separately. In regions where the nervous tissue is found to be isotropic these are reduced to the three components of the vector grad $\sigma(x)$. Thus, the components $d\sigma/dx_i$ were determined in various animals in the surrounding of the acoustic neuropile of the mesothoracic ganglion since this region is supposed to be isotropic. Some examples of relative conductivities according to the actual mean values σ_i for different single animals are shown in Fig. 4a–c. The zero values given at the abcissa indicate only relative positions, since the actual absolute position of the electrode set could not be determined precisely. In the x-direction the position of the most lateral electrode was taken as the reference ($x = 0$), in the y-direction the most frontal electrode ($y = 0$) and in

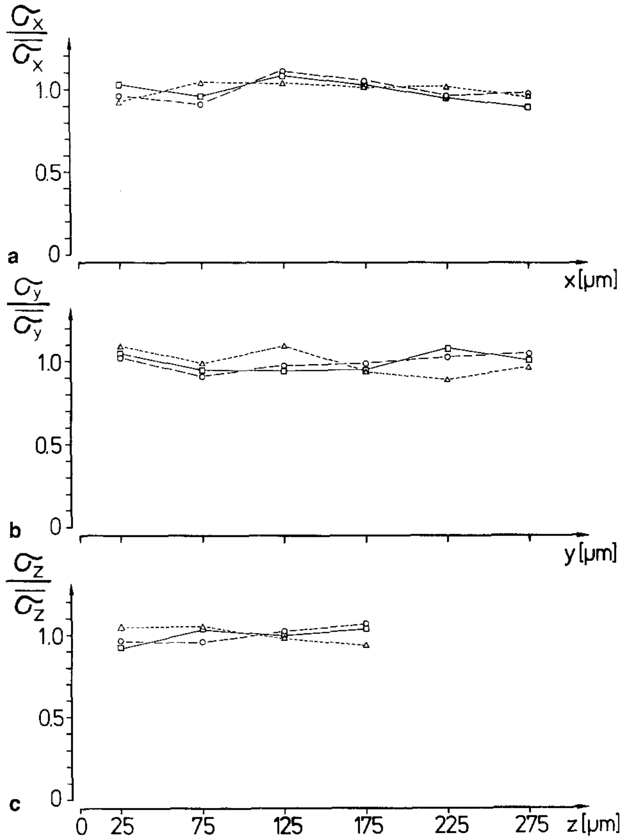

Fig. 4a–c. Relative conductivities from three experiments as a function of the three directions of space in different single animals. $\bar{\sigma}_i$: actual mean value. The zero values at the abcissa only represent relative positions (see text). **a** x-direction, **b** y-direction, **c** z-direction

the z-direction the upper (most ventral) electrode ($z = 0$). In the latter case only five electrodes were assembled due to experimental limitations caused by the electrode arrangement with respect to the penetration axis (z-axis).

In any direction, σ remains constant and no significant dependence on $\vec{\mathbf{x}}$ was revealed. Thus, within the investigated range of space the tissue is approximately homogenous [grad $\sigma(\vec{\mathbf{x}}) \approx 0$].

Discussion

In the locust, the conductivities were found to be about 0.4 mS/cm within the thoracic ganglia. This value is considerably smaller than in vertebrate nervous tissue, e.g., in the molecular layer of the cat cerebellum:

$$\sigma_x = (3.3 \pm 0.7)\ \text{mS/cm};\ \sigma_y = (1.7 \pm 0.3)\ \text{mS/cm};$$
$$\sigma_z = (2.8 \pm 0.7)\ \text{mS/cm}$$

(Yedlin et al. 1974).

The reasons for these differences were not investigated in more detail. Smaller extracellular space (interstitium) and/or greater membrane resistivities may be assumed to be the cause of this magnitude of difference.

In some brain structures, as for instance in the molecular layer of the cerebellum, anatomical features may reveal an intrinsic coordinate system according to preference directions due to certain orientations of the neuronal elements in this tissue. Kwan and Murphy (1974) have shown that with a proper choice of such a coordinate system the off-diagonal elements of the conductivity tensor become zero. The diagonal elements represent values along mutually orthogonal axes (along the parallel fibers, normal to the cortical surface and orthogonal to these axes). Hence, in contrast to our experiments the directions of anisotropies are known from the outset. However, for all those cases where no morphologically apparent anisotropy directions are present, the method developed in this paper yields a reliable means of determining intrinsic coordinate systems biophysically.

Within the vertebrate cerebellum, the degree of anisotropy is considerable and the conductivities of various directions may differ several times [in *Rana catesbeiana* Nicholson and Freeman (1975) found differences up to five times]. This also is a consequence of the high degree of neuronal arrangement creating preference directions with respect to current flow. In contrast, the anisotropy within the acoustic neuropile of the metathoracic ganglion (Th_3) of *Locusta migratoria* is only very weak. The arrangement of the neuronal elements involved is diffuse although functionally (primary synaptic transmission of acoustic information) the region of the acoustic neuropile seems to be a well-limited area when only the presynaptic receptor terminals are considered (shown in Fig. 2). Thus, one could expect certain structural orientations or borderlines causing inhomogenities and anisotropies. It becomes clear, however, that this is not the case when considering also postsynaptic elements running out of this area and crossing this pretended bordered region. Furthermore, these regions often represent different sensory modalities (i.e., vibratory inputs at the dorsal part of the neuropile) and various receptor projection areas overlap instead forming independent structures. Thus, such presumed limited synaptic areas cannot be revealed and the electrical properties of neuropiles may not correlate to the functional ones.

Although when choosing a coordinate system (according to Fig. 2) even slight anisotropies should be considered, in practice (for example field potential analysis, current source density analysis etc.) the assumption of isotropy ($\sigma_x \approx \sigma_y \approx \sigma_z$) constitutes a sufficient approximation (Breckow et al. 1982).

The efficiency of this method is particularly evident in diffusely arranged tissues without any obviously preferential axes. A further estimation of the sensibility, however, would be possible by measurements in structured tissues (i.e., with marked anisotropies).

The validity of Eqs. (8)–(15) is only given in particular for an infinite medium. This means, the electrical field generates spherical equi-potential planes concentrical around the current injecting electrode tip. The ganglion surface represents a surface boundary with respect to these equi-potential planes, distorting their spherical spreading dependent on the distance between current electrode tip and ganglion surface. Hence, when sampling the potential distribution generated at a current point $\vec{x}_0$ one has to take care that the spherical form of the equi-potential planes at the potential recording point is fulfilled. Thus, the range within which this assumption is fulfilled depends on the relationship between the depth of the current injection point and the distance Δx to the potential recording point. In our experiments, the depths were about 100 μm . . . 200 μm. An estimation shows that surface boundary effects for distances not greater than $\Delta x = 50$ μm . . . 100 μm can be neglected. For greater distances influences from boundary effects were measured and result in a limitation of the available electrode distance Δx to $h = 50$ μm and $2\ h = 100$ μm according to the configuration of Fig. 1b.

Errors may be introduced mainly by possible existing inhomogenities within small distances (< 50 μm) and by incorrect electrode positioning. The latter is discussed in Breckow et al. (1982). The electrode tip distances were measured with the microscope. Their variations from the standard distances (50 μm, 100 μm, . . .) were normally less than 5 μm. The conductivities were, however, calculated with these actual distances. Inhomogenities along short distances cannot be excluded. However, results with the electrode configuration shown in Fig. 1a for σ_z at various depths with step widths of about 20 μm show no significant σ-differences. This may justify the assumption of homogenity also below 50 μm.

Since proper evidence from extracellular (field) potentials of neuronal ensemble activities cannot be developed without knowledge of the underlying current flows (Nicholson 1973) it is desirable to have a reliable method for the convenient invesigation of the electrical properties. The present paper gives one approach for a conductivity measuring technique allowing investigation of conductivity properties, inhomogenities and anisotropies in a nervous tissue without any assumptions with regard to structure, function, and anatomy.

Acknowledgements. We are very grateful to Prof. K. Kalmring for his critical discussion and to Dr. R. Kühne and Dr. S. Silver for improving the English text. Mrs. E. Schäfer and Mr. H. Schmidt supported this study by technical help and Mr. J. Weitkämper performed the extensive computer calculations.

References

Breckow J, Kalmring K, Eckhorn R (1982) Multichannel-recordings and real-time current source density (CSD) analysis in the central-nervous system of insects. Biol Cybern 45: 115–121

Freeman JA, Nicholson C (1975) Experimental optimization of current source-density technique for anuran cerebellum. J Neurophysiol 38: 369–382

Freeman JA, Stone J (1969) A technique for current density analysis of field potentials and its application to the frog cerebellum. In: Llinas R (ed) Neurobiology of cerebellar evolution and development. American Medical Association, Chicago, IL, pp 412–430

Joos G (1977) Lehrbuch der theoretischen Physik. Akademische Verlagsgesellschaft, Wiesbaden

Kwan HC, Murphy JT (1974) A basis for extracellular current density analysis in cerebellar cortex. J Neurophysiol 37: 170–180

Landau LD, Lifschitz EM (1960) Electrodynamics of continuous media. Addison-Wesley, Reading, MA

Morse PM, Feshbach H (1963) Methods of theoretical physics. McGraw-Hill, New York

Nicholson C (1973) Theoretical analysis of field potentials in anisotropic ensembles of neuronal elements. IEEE Trans Biomed Eng 20: 278–288

Nicholson C, Freeman JA (1975) Theory of current source-density analysis and determination of conductivity tensor for anuran cerebellum. J Neurophysiol 38: 356–368

Yedlin M, Kwan H, Murphy JT, Nguyen-Huu H, Wong YC (1974) Electrical conductivity in cat cerebellar cortex. Exp Neurol 43: 555–559

Received June 6, 1983/Accepted October 10, 1983